Selective Optical Control of Electron Spin Coherence in Singly Charged GaAs-$Al_{0.3}Ga_{0.7}As$ Quantum Dots

Yanwen Wu,[1] Erik D. Kim,[1] Xiaodong Xu,[1] Jun Cheng,[1] D. G. Steel,[1,*] A. S. Bracker,[2] D. Gammon,[2] Sophia E. Economou,[3,†] and L. J. Sham[3]

[1]*The H. M. Randall Laboratory of Physics, University of Michigan, Ann Arbor, Michigan 48109, USA*
[2]*The Naval Research Laboratory, Washington D.C. 20375, USA*
[3]*Department of Physics, University of California, San Diego, La Jolla, California, 92093-0319, USA*

(Received 22 February 2007; published 29 August 2007)

Coherent transient excitation of the spin ground states in singly charged quantum dots creates optically coupled and decoupled states of the electron spin. We demonstrate selective excitation from the spin ground states to the trion state through phase sensitive control of the spin coherence via these three states, leading to partial rotations of the spin vector. This progress lays the ground work for achieving complete ultrafast spin rotations.

DOI: 10.1103/PhysRevLett.99.097402 PACS numbers: 78.67.Hc, 42.50.Hz, 42.50.Md, 71.35.Pq

The two spin states of an electron inside a semiconductor quantum dot (QD) can be mapped directly to the two operational states in quantum information processing. The lifetime of the spin states is on the order of milliseconds [1–3], making the electron spin an ideal realization of a quantum bit (qubit). Electron spin rotations have already been demonstrated in surface gated dots using electrical gates [4], but the operation time is limited to a few microseconds by the microwave control resonant with the spin states. Alternatively, ultrafast optical pulses are readily available. Manipulating the spin states with these pulses increases the gate operation speed and hence the number of operations during the spin coherence lifetime. Fast operation rates are crucial for practical quantum information processing.

In this Letter, we demonstrate phase sensitive partial rotations of the electron spin vector in an ensemble of singly charged QDs using picosecond pulses. Similar rotations have been performed on electrons in quantum wells [5,6]. The rotations are achieved through optically coupling the spin ground states to the charged exciton (trion) state. The accomplishment of the partial rotations prepares the way for the demonstration of complete rotations of a single spin, which would encompass arbitrary qubit rotations.

The sample used in this study contains an ensemble of interface fluctuation GaAs/$Al_{0.3}Ga_{0.7}As$ QDs (IFQD) [7–9] charged with single electrons through modulation silicon δ-doping. The number of electrons in each dot is determined by the doping density of the sample. In this case, the doping density is $10^{10}/cm^2$, which gives an average of one electron per dot [10]. The sample is placed inside a magnetic cryostat cooled to 5 K. The magnetic field applied in the experiments is aligned in the Voigt geometry, perpendicular to the sample growth axis, z. The magnitude of the field is fixed at $B = 6.6$ T.

The population and coherence decay times in these QDs range from 30 ps for the trion population to a T_2^* of about 400 ps for the ensemble spin coherence at $B = 6.6$ T [11]. As a compromise between temporal and spectral resolution, 3 ps pulses are chosen for the experiments. Three pulses are used to excite, control, and measure the QD system, denoted as the pump pulse, the control pulse with tunable delay (τ_c) and pulse area (θ_c), and the temporally scanning probe pulse. The pump and probe pulses are each modulated at 1 MHz and 1.05 MHz, respectively, while the control pulse is unmodulated. The nonlinear optical signal in differential transmission (DT) is homodyne-detected along the probe path at the difference frequency of 50 kHz.

The energy structure of the singly charged QD at $B = 0$ T can be described by two degenerate two-level systems, each consisting of one spin ground state and one trion excited state, as shown in Fig. 1(a). The total angular momentum projections along the z axis of the spin ground

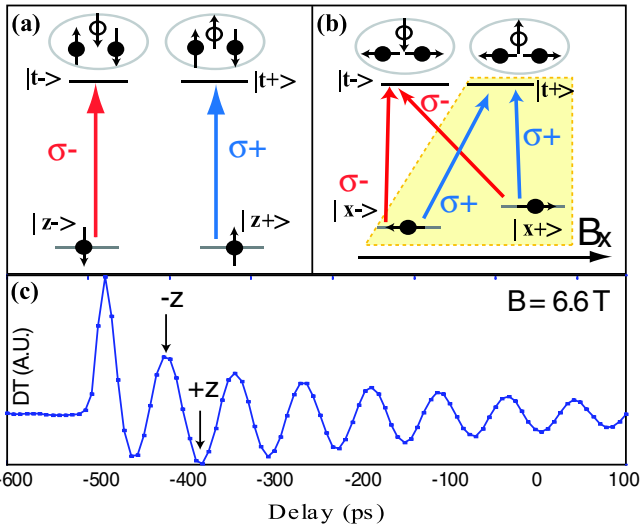

FIG. 1 (color online). Energy level diagrams of a charged QD at (a) $B = 0$ T and (b) $B \neq 0$ T in the Voigt geometry. (c) Two-beam (pump and probe) quantum oscillation signal of the initialized spin polarization at $B = 6.6$ T.

states $|z\pm\rangle$ are $\pm\frac{1}{2}$, defined by the electron spin, while those of the singlet trion states $|t\pm\rangle$ are $\pm\frac{3}{2}$, defined by the hole spin. The electron spins do not contribute to the total angular momentum of the trion due to the antipairing. The allowed optical transitions are then restricted to $\triangle m = \pm 1$ for $\sigma_\pm$ polarized excitations. This angular momentum restriction inhibits optical coupling between the two spin states.

Indirect optical coupling between the spin states is enabled by applying a magnetic field in the Voigt geometry, which produces two new eigenstates of the electron spin, $|x\pm\rangle = (|z+\rangle \pm |z-\rangle)/\sqrt{2}$ parallel or antiparallel to $\vec{x}$, the magnetic field direction [Fig. 1(b)]. The in-plane electron g factor in this sample is 0.13 [9,12], and thus the Zeeman splitting is approximately $\Delta \sim 50\ \mu$eV at 6.6 T.

In contrast, the highly suppressed mixing of the light and heavy hole states at even 6.6 T by the strong spin orbital coupling in this particular sample leads to a negligibly small in-plane hole g factor [9]. This causes the hole spins to be pinned along the z axis. Consequently, the trion states remain unaffected by the magnetic field. The spin ground states are now optically coupled through the trion states by either σ_+ or σ_- polarized optical pulses. Since the two Λ systems are essentially equivalent, without loss of generality, we concentrate on the σ_+ polarized Λ system highlighted in Fig. 1(b).

In the presence of the σ_+ pulses, stimulated Raman transitions are driven through the trion state $|t+\rangle$. The σ_+ pulses have a bandwidth of $\Omega \sim 400\ \mu\text{eV} \gg \Delta$, which couple both spin states, $|x\pm\rangle$, to $|t+\rangle$ simultaneously and equally. The equations of motion in the field interaction representation are then

$$\dot{C}_{|x+\rangle} = -i\chi * C_{|t+\rangle}, \qquad \dot{C}_{|x-\rangle} = -i\chi * C_{|t+\rangle}, \qquad \dot{C}_{|t+\rangle} = -i\chi(C_{|x+\rangle} + C_{|x-\rangle}), \tag{1}$$

where the C's are the probability amplitudes of the different states and χ is the optical field. Two optically coupled and decoupled states, $|z\pm\rangle = (|x+\rangle \pm |x-\rangle)/\sqrt{2}$, are formed for the σ_+ polarization chosen. The $|z-\rangle$ state has no χ dependence, indicating that it is completely decoupled from the optical field. Conversely, $|z+\rangle$ is fully coupled to the σ_+ optical excitation. Spin initialization and polarization control are achieved utilizing this state pair. Decay terms are not included in the equations as long as the pulse duration is short compared to the trion and spin decay times. For evolution of the system after the pulses, trion decay is important, as discussed later.

At a temperature of 5 K, the thermal excitation energy is 430 μeV, which is an order of magnitude larger than the electron Zeeman splitting energy, Δ. This results in a completely mixed state of the electron spin, which also means equal population in both spin ground states and zero spin coherence in any basis. This completely mixed spin subspace is inoperable using only unitary transformations within this two-level system.

The initialization of the spin out of the completely mixed state is accomplished with a single pump pulse. A probe pulse reads out the result. The pump pulse transfers population from state $|z+\rangle$ to the trion $|t+\rangle$ state, leaving a net population difference of magnitude ξ in the optically decoupled state $|z-\rangle$. This population difference in the spin subspace signifies a net spin polarization in the $-\vec{z}$ direction. The net spin polarization precesses at the Larmor frequency, $\omega_L = \frac{\Delta}{\hbar}$, around the magnetic field in the z-y plane, corresponding to population cycling through the $|z\pm\rangle$ states. The beat signal in Fig. 1(c) traces the projected magnitude of the spin polarization along $\vec{z}$, the optical readout axis. The peaks and troughs of the beats represent net spin polarization pointing along the $-\vec{z}$ (spin population in the $|z-\rangle$ state) and $\vec{z}$ (spin population in the $|z+\rangle$ state) directions, respectively.

The density matrix ρ_z in the z basis after initialization and trion decay can be written as a sum of the coherent and incoherent components in the absence of spin relaxation.

$$\rho_z = \rho_{\text{inc}} + \rho_{\text{coh}} = \begin{bmatrix} \frac{1-\xi}{2} & 0 \\ 0 & \frac{1-\xi}{2} \end{bmatrix} + \xi \begin{bmatrix} \cos^2\frac{\omega_L\tau}{2} & \frac{i}{2}\sin\omega_L\tau \\ \frac{-i}{2}\sin\omega_L\tau & \sin^2\frac{\omega_L\tau}{2} \end{bmatrix} \tag{2}$$

where the delay time τ is measured from a peak of the Larmor oscillations. The incoherent part of the density matrix ρ_{inc} describes the equal distribution of the uninitialized spin population $1-\xi$ between the $|z\pm\rangle$ states. The coherent part ρ_{coh} describes the time evolution of the initialized spin population ξ. The initialized spin polarization with unit $\hbar/2$ in Cartesian coordinates is then given by

$$\vec{S}_{\text{coh}} = \xi(0, -\sin\omega_L\tau, \cos\omega_L\tau) \tag{3}$$

representing the precession of the spin vector around the x axis on the z-y plane.

We note here that at 6.6 T, the contribution from spontaneously generated coherence (SGC) [11] is negligible in the initialization process. The maximum initialized population is 0.5 via a π pulse excitation to the trion. A more detailed discussion of the initialization process has been reported theoretically [13] and experimentally [12] using multiple pump pulses. The ensemble spin coherence time of about 400 ps at 6.6 T is limited by the inhomogeneous broadening of the electron g factor and the spectral diffusion process.

The initialized spin polarization described by ρ_{coh} can now be controlled through an optical pulse. Arbitrary rotations of the spin are achieved through selective excitations at different positions on the z-y plane during the precession of the net spin polarization. By controlling this excitation, we can control both the relative population and phase between the $|z\pm\rangle$ components in the pure state. If the optical field performs a coherent Rabi rotation on $|z+\rangle$ via the trion and back with a net phase change, ϕ, a general spin state, $|\psi\rangle$, will have the phase change in its $|z+\rangle$ component without affecting its $|z-\rangle$ component, i.e.,

its spin vector rotates about the z axis. The general spin state for the initialized and properly controlled spin polarization has the form

$$|\psi\rangle = \sqrt{\xi}\left[e^{i\phi} \cos\frac{\omega_L \tau}{2} |z+\rangle - i \sin\frac{\omega_L \tau}{2} |z-\rangle \right] \quad (4)$$

where ϕ is the net phase between states $|z\pm\rangle$ induced by the control pulse. For $\omega_L \tau = \frac{\pi}{2}$ and $\phi = \mp\frac{\pi}{2}$, the spin state $|\psi\rangle$ is proportional to $|x\pm\rangle$ along the x axis. Similarly, a zero or π value of ϕ puts the spin state in $|y\pm\rangle$ along the y axis. If the optical Rabi rotation is π, bringing state $|z+\rangle$ to the trion state, followed by the trion decaying equally to the $|x\pm\rangle$ states thus annihilating a portion of the spin coherence, then the net result is a rotation together with a reduction of the magnitude of the spin vector. This is a partial rotation.

We first consider using a pulse area $\theta_c = \pi$ control pulse delayed at different τ_c from the pump pulse to rotate the initialized spin polarization at different times during the Larmor precession. When the control pulse arrives at $\tau_c = \tau_{+z} = \frac{\pi}{\omega_L}$, the entire initialized spin population ξ is in state $|z+\rangle$ as shown in Fig. 2(a). The π pulse excites all of ξ from $|z+\rangle$ to the trion state $|t+\rangle$. After the decay of $|t+\rangle$, the system returns to the completely mixed state, as the excited population ξ redistributes equally and incoherently between the two spin ground states. As a result, the quantum beats are annihilated and the simulated signal exhibits

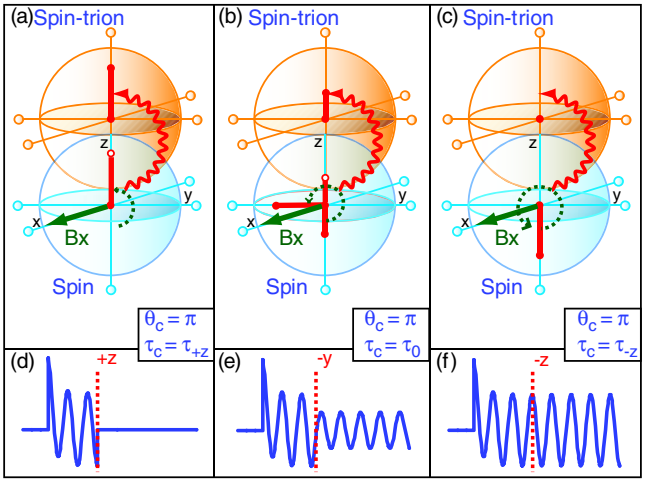

FIG. 2 (color online). Evolution of the spin polarization vector at control pulse delays of (a) $\tau_c = \tau_{+z}$, (b) $\tau_c = \tau_0$, and (c) $\tau_c = \tau_{-z}$. The upper (lower) sphere is the trion-spin (spin) subspace. The zig-zagged lines represent the σ_+ polarized optical control field. The solid arrows indicate the magnetic field directions, and the dotted curves are the paths of the precession of the spin polarization vector prior to the arrival of the control pulse. The solid bars represent the spin polarization alignment. (d), (e), and (f) are simulated quantum oscillation signals before and after the control pulse at the different τ_c indicated in (a), (b), and (c), respectively.

a flat line following the control pulse at $\tau_c = \tau_{+z}$ as shown in Fig. 2(d).

By moving the control pulse to $\tau_c = \tau_0 = \frac{3\pi}{2\omega_L}$, where the optical signal or the z component of the spin polarization is zero as shown in Fig. 2(b), the spin polarization is along $-\vec{y}$, and states $|z\pm\rangle$ have equal populations. The oscillation amplitude is decreased by half after the control pulse as expected in Fig. 2(e) because half of ξ is being "protected" in state $|z-\rangle$ and is not destroyed by the decay and redistribution process.

Finally, when the spin polarization is along $-\vec{z}$ at $\tau_c = \tau_{-z} = \frac{2\pi}{\omega_L}$, all of ξ is preserved in the optically decoupled state $|z-\rangle$ as illustrated in Fig. 2(c). The quantum beats are unaffected by the control pulse and continue to oscillate uninterrupted as pictured in Fig. 2(f).

Overall then, as this delay τ_c of the control optical pulse is scanned, the beat amplitude, which is also the magnitude of the spin polarization $|\vec{S}(\tau_c)|$ from Eq. (3) after the control pulse, follows an oscillatory behavior

$$|\vec{S}_{\text{coh}}(\tau_c)| = \frac{\xi}{2}(1 + \cos\omega_L \tau_c). \quad (5)$$

This discussion has treated the optical excitations and precession dynamics in the magnetic field separately. The assumption is valid since the temporal pulse width (3 ps) is much shorter than the oscillation period of the quantum beats (85 ps). Therefore, we can approximate the excitation to the trion state as instantaneous so that precession around the magnetic field during the optical pulse duration is negligible.

Experimentally, we need to consider the effect of the control on the uninitialized population in addition to the initialized population. In the two-frequency modulation spectroscopy used in the experiments, the DT signal detected at the difference modulation frequency is equivalent to the signal taken with the pump pulse on minus pump pulse off. When the pump beam is off, the $\theta_c = \pi$ control pulse produces quantum beats with an amplitude of $|\vec{S}_{\text{off}}| = \frac{1}{2}$ from the completely mixed spin states, regardless of the control delay τ_c. However, when the pump pulse is turned on, the position of the control delay τ_c becomes significant. The beat amplitude after both the pump and control pulses consists of two terms, where the first is a τ_c dependent controlled term, $|\vec{S}_{\text{coh}}(\tau_c)|$, due to both the pump and control pulses as described in Eq. (5), and the second term is a noncontrolled term, $|\vec{S}_{\text{inc}}| = \frac{1-\xi}{2}$, due to the redistributed uninitialized spin population. The final amplitude of the normalized quantum beat signal detected after the control pulse, determined by the function $I_{\text{on-off}}$ for pump pulse on minus off, is the sum of the controlled ($|\vec{S}_{\text{coh}}(\tau_c)|$) and noncontrolled terms ($|\vec{S}_{\text{inc}}|$) minus $|\vec{S}_{\text{off}}|$,

$$I_{\text{on-off}}(\tau_c) = \frac{\xi}{2} \cos\omega_L \tau_c. \quad (6)$$

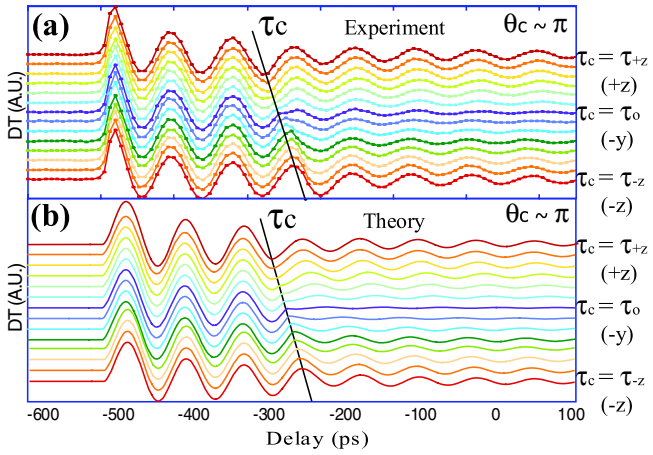

FIG. 3 (color online). (a) Experimental result of the three-beam (initialization, control, and probe) quantum oscillation signal at different control delays τ_c. The solid line indicates the position of the control pulse. (b) Theoretical simulations of the same experimental set up in (a).

Data of the three-beam control experiment are shown in Fig. 3(a). The $\cos\omega_L\tau_c$ dependence observed in the signal beat amplitudes after τ_c (solid line) in Fig. 3(a) is in contrast with the $1 + \cos\omega_L\tau_c$ dependence of the physical pictures in Figs. 2(d)–2(f) as anticipated in Eq. (6). For example, at $\tau_c = \tau_{+z}$, Fig. 2(d) shows vanishing quantum beats after τ_c, while the quantum beat signal corresponding to $\tau_c = \tau_{+z}$ in Fig. 3(a) persists due to the nonzero $I_{\text{on-off}}$. Numerical simulations in Fig. 3(b) take into account the experimental parameters, such as the pulse width, beam modulations, and decoherence times of the system. The theoretical results are in excellent agreement with the experiment.

We note that unlike the work in Ref. [12], where the observed signal is a result of the quantum interference between two independently initialized spin coherences induced by the pump and control pulses, the behavior described here is due to the subsequent rotation by the control pulse of the actual pump-induced spin coherence. In terms of optical pulses as transformation matrices for the state vector of the quantum system, the former is a sum of two matrices while the latter is a product.

To completely control the rotations of the electron spin in the spin subspace without populating the trion, we need to use a $\theta_c = 2\pi$ pulse to control the relative phase ϕ between states $|z\pm\rangle$ in addition to the populations. This phase control performs a complete Rabi rotation of state $|z+\rangle$. As a result, the population in $|z+\rangle$ is unaffected by the 2π pulse, but the state gains an overall phase depending on the detuning of the pulse from the trion state [14]. For example, the overall phase gained for an on resonance 2π control pulse is $\phi = \pi$. At $\tau_c = \tau_0$, the spin state is rotated from $|y-\rangle$ to $|y+\rangle$, representing a spin flip. Similarly, $\phi = \frac{\pi}{2}$ rotates the spin state from $|y-\rangle$ to $|x+\rangle$. The magnetically induced Larmor precession about $\vec{x}$ and optically induced rotation about $\vec{z}$ are sufficient for creating any arbitrary spin state. For an all-optical ultrafast spin rotation scheme, optically induced rotation around $\vec{x}$ [15] can replace the Larmor precession.

Our data shows a partial rotation. The reason for the limitation in IFQDs, namely, the difficulty in completing a trion Rabi rotation, is not fully understood, especially in light of the fact that Rabi oscillations in neutral IFQDs have been observed [16]. However, the demonstration of Rabi oscillations of trions in self-assembled QDs [3] shows that the result in this experiment should be readily applicable in those structures.

This work was supported in part by NSF, FOCUS, DARPA, NSA/ARO, and ONR.

*dst@umich.edu
†Present address: Naval Research Laboratory, WA, DC 20375, USA

[1] M. Kroutvar, Y. Ducommun, D. Heiss, M. Bichler, D. Schuh, G. Abstreiter, and J. J. Finley, Nature (London) **432**, 81 (2004).
[2] J. M. Elzerman, R. Hanson, L. H. W. van Beveren, B. Witkamp, L. M. K. Vandersypen, and L. P. Kouwenhoven, Nature (London) **430**, 431 (2004).
[3] A. Greilich, R. Oulton, E. A. Zhukov, I. A. Yugova, D. R. Yakovlev, M. Bayer, A. Shabaev, A. L. Efros, I. A. Merkulov, and V. Stavarache *et al.*, Phys. Rev. Lett. **96**, 227401 (2006).
[4] F. H. L. Koppens, C. Buizert, K. J. Tielrooij, I. T. Vink, K. C. Nowack, T. Meunier, L. P. Kouwenhoven, and L. M. K. Vandersypen, Nature (London) **442**, 766 (2006).
[5] J. A. Gupta, R. Knobel, N. Samarth, and D. D. Awschalom, Science **292**, 2458 (2001).
[6] Y. Shen, A. M. Goebel, and H. Wang, Phys. Rev. B **75**, 045341 (2007).
[7] D. Gammon, E. S. Snow, B. V. Shanabrook, D. S. Katzer, and D. Park, Phys. Rev. Lett. **76**, 3005 (1996).
[8] D. Gammon, E. S. Snow, B. V. Shanabrook, D. S. Katzer, and D. Park, Science **273**, 87 (1996).
[9] J. G. Tischler, A. S. Bracker, D. Gammon, and D. Park, Phys. Rev. B **66**, 081310(R) (2002).
[10] A. S. Bracker, E. A. Stinaff, D. Gammon, M. E. Ware, J. G. Tischler, D. Park, D. Gershoni, A. V. Filinov, M. Bonitz, and A. V. Filinov *et al.*, Phys. Rev. B **72**, 035332 (2005).
[11] M. V. G. Dutt, J. Cheng, B. Li, X. Xu, X. Li, P. R. Berman, D. G. Steel, A. S. Bracker, D. Gammon, and S. E. Economou *et al.*, Phys. Rev. Lett. **94**, 227403 (2005).
[12] M. V. G. Dutt, J. Cheng, Y. Wu, X. Xu, D. G. Steel, A. S. Bracker, D. Gammon, S. E. Economou, R.-B. Liu, and L. J. Sham, Phys. Rev. B **74**, 125306 (2006).
[13] A. Shabaev, A. L. Efros, D. Gammon, and I. A. Merkulov, Phys. Rev. B **68**, 201305(R) (2003).
[14] S. E. Economou, L. J. Sham, Y. Wu, and D. G. Steel, Phys. Rev. B **74**, 205415 (2006).
[15] C. Emary and L. J. Sham, J. Phys. Condens. Matter **19**, 056203 (2007).
[16] T. H. Stievater, X. Li, D. G. Steel, D. Gammon, D. S. Katzer, D. Park, C. Piermarocchi, and L. J. Sham, Phys. Rev. Lett. **87**, 133603 (2001).